UNIAXIAL DEFORMATION OF RUBBER CYLINDERS

P. H. MOTT AND C. M. ROLAND

CHEMISTRY DIVISION, CODE 6120, NAVAL RESEARCH LABORATORY, WASHINGTON, D.C. 20375-5342

ABSTRACT

Stress, strain and optical birefringence measurements were made on elastomeric cylinders deformed in tension and compression. The birefringence data enables the actual stress to be determined even when the deformation is not homogeneous. In the absence of lubricant, uniaxially loaded rubber cylinders deviate from homogeneous deformation due to bonding of the cylinder ends. The existing analysis to correct the force–deflection curve for the effect of this sticking, strictly valid for infinitesimal strains, is premised on the idea that the deformed cylinder has a parabolic profile. Experimentally, however, it was found that slender rubber cylinders assume a much flatter profile, while maintaining constant volume, when deformed. Nevertheless, the accuracy of the stress–strain curve when the standard correction is applied turns out to be quite good, partially a result of cancellation of two, relatively small, errors. This accuracy was assessed by comparison of force–deflection data from bonded cylinders both to stress–strain data obtained on lubricated cylinders and to the stresses deduced from the measured birefringence.

INTRODUCTION

The compression of blocks is often employed in the mechanical characterization of elastomers due to the ease of the method. However, soft rubber adheres to the confining plates, so that the resulting deformation is not homogeneous compression; some correction of the force–deflection curve is required to obtain the actual rubber modulus. Analyses of the compression, bending and shear of bonded rubber blocks have been carried out, principally by Gent and coworkers,[1-6] demonstrating how geometry-independent material properties can be extracted from such data.

In this paper we report stress, strain and birefringence measurements carried out on uniaxially deformed rubber cylinders having various aspect ratios.

EXPERIMENTAL

Deproteinized natural rubber (H. A. Astlett Co.), which is more transparent than ordinary *Hevea*, and a 1,4-polybutadiene (Goodyear Tire & Rubber Co.'s Budene 1209) were used. The polymers were mill-mixed, then compression molded for either 30 minutes at 160°C (NR) or 120 minutes at 150°C (BR). The cylinder diameters were always 12.3 mm, while the height was varied from 11.3 mm to 28.8 mm ($0.92 < \text{aspect ratio} < 2.3$). The crosslink densities of the samples, calculated from Young's modulus,[7] are given in Table I.

The apparatus used to obtain the force–deflection data is depicted in Figure 1. The sample was positioned between a polarizer and a quarter-wave plate, both of which were oriented $\pi/4$ radians to the direction of the applied load. The birefringence was measured by rotation of a second polarizing filter (the analyzer), initially oriented perpendicular to the first polarizer, to minimize the intensity of the transmitted light. The birefringence Δn is given by[8]

$$\Delta n = \frac{\theta}{\pi} \cdot \frac{\lambda}{2r}, \tag{1}$$

where λ is the wavelength of the HeNe laser (632.8 nm) and θ is the rotation of the analyzer, which reached values as high as 20π in these experiments. The path length of the light through the sample, $2r$, corresponds to the maximum bulge diameter $2R_{max}$ of the compressed cylinder. This was measured by translating the sample horizontally, and identifying the cylinder outer surfaces when the transmitted intensity fell to one-half of the intensity when the beam missed the sample. The vertical profile of the squeezed cylinders was determined in a similar fashion.

TABLE I

ELASTOMER COMPOUNDS

	NR-1	NR-2	BR-1
Deproteinized NR	100	100	—
1,4-Polybutadiene	—	—	100
Dicumyl peroxide	1.0	2.0	0.441
Antioxidant[a]	—	—	1.015
Young's modulus (MPa)	0.89	1.46	2.16
Crosslink density (moles/m^3)[b]	120	200	290
C (GPa^{-1})[c]	2.07	2.04	3.58

[a] 1,2-dihydro-2,2,4-trimethylquinoline
[b] Calculated from the modulus as E/3RT.[7]
[c] Stress-optical coefficient.

All results herein correspond to mechanical equilibrium. Typically two measurements per day were possible for the BR; equilibrium data could be acquired somewhat faster for the more rapidly relaxing NR. The change in height ΔH of the sample was measured with a linear voltage differential transducer (LVDT). The engineering strain is then $\epsilon = \Delta H/H_0$, where H_0 was the height of the unloaded cylinder. The engineering stress is the force per initial cross-sectional area, $\sigma_{eng} = F/\pi R_0^2$, where F is the applied load and R_0 the radius of the unloaded cylinder.

In addition to the compression experiments, extension measurements were carried out by inverting the apparatus in Figure 1. To verify the repeatability of the data as the load changes sign, the sample was also extended while in the compression geometry by means of a screw pulling up on the loading stage. The stress was then determined from Brewster's Law[7,8]

$$\sigma = \frac{\Delta n}{C}, \tag{2}$$

where C is the stress-optical coefficient and σ is the true stress, $\sigma = F/\pi R_{max}^2$. These "bridging"

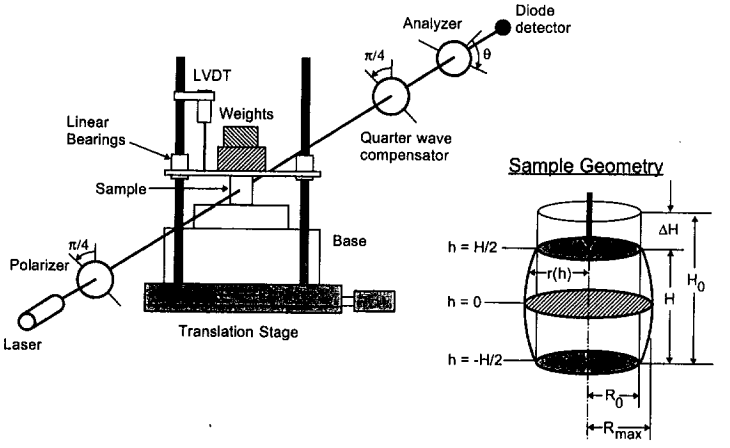

FIG. 1.—The experimental apparatus used for simultaneous force and birefringence measurements on rubber cylinders uniaxially compressed and extended. To obtain data for extended cylinders, the load apparatus was inverted. To obtain data bridging the vicinity of $\epsilon = 0$, the extension was carried out in the compression configuration, with the strain imposed by a screw pulling up on the weight stage and the stress determined from the birefringence.

experiments rely on the invariance of the stress-optical coefficient to strain at small deformations.

Bonding of the cylinders to the Al plates was assured by gluing (cyanoacrylate adhesive). Experiments in compression were also carried out with slipping at the cylinder ends, achieved by introducing silicone oil between the rubber and the metal plate. An absence of sticking was confirmed by measurements of the cylinder diameter while under load.

RESULTS AND ANALYSIS

At small strains, deformation of bonded rubber cylinders of height H and radius r will produce a parabolic profile parallel to the stretch direction[1]

$$r(h) = (R_0 - R_{max})\left(\frac{2h}{H}\right)^2 + R_{max}, \tag{3}$$

where h is the distance along the vertical direction, measured from the center (see Figure 1). The lateral contraction (or bulge) at the center is given by[2]

$$R_{max} = R_0\left(1 - \frac{3}{4}\epsilon\right). \tag{4}$$

Bonding of the rubber implies no slip at the ends [that is, $r(\pm H/2) = R_0$ in Figure 1], which causes shear strains to develop, as experimentally verified by Gent.[3] These shearing forces increase the stiffness of the cylinder, with the engineering stress then given by[5]

$$\sigma_{eng} = E\epsilon\left(1 + \frac{R_0^2}{2H_0^2}\right), \tag{5}$$

where E is the Young's modulus of the rubber. Although strictly valid only for low aspect ratio cylinders,[2] the analysis is useful over a substantial range of geometries since the correction term $R_0^2/2H_0^2$ in Equation (5) is small for slender cylinders. For slender cylinders, the analysis underlying Equations (3–5) is in error in the assumption of a parabolic profile, since the effect of bonding is restricted to the end regions. Additionally, Equation (4) does not provide for volume conservation. These discrepancies are seen in Figure 2, where the radius measured along the vertical direction of a compressed cylinder is much flatter than

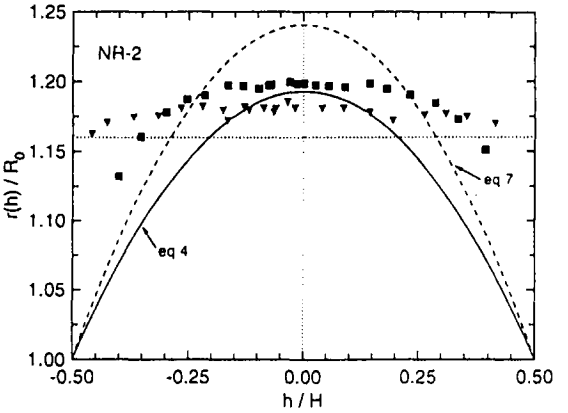

FIG. 2.—The bulging of a bonded cylinder expressed as the radius r divided by the initial (uncompressed) radius R_0 for NR-2 at a compressive strain of 26% (glued ends ■■■; without adhesive ▼▼▼) as a function of the normalized height h/H. Both curves were calculated assuming a parabolic profile [Equation (3)]; the dashed curve was calculated assuming incompressible rubber [Equation (7)], while the solid curve represents the Gent prediction [Equation (4)]. The dotted horizontal line corresponds to the radius for a nonbonded disk (complete slippage induced by lubrication) at the same strain. Note that without lubricant present, the absence of adhesive does not result in much slippage.

parabolic. Moreover, the profile calculated using Equations (3) and (4) substantially underestimates the volume (for example, by 4.8% at 25% compressive strain). Of course, this error is diminished in the limit of infinitesimal strains. Note in Figure 2 that although an adhesive was usually used to prevent slipping, the profile of the cylinder hardly changes if the adhesive is omitted; the neat rubber adheres well to the confining metal plates.

We can modify Equation (4) to obtain a solution consistent with no volume change upon deformation. Retaining the assumption of a parabolic profile, the unstrained and strained volumes are set equal:

$$R_0^2 H_0 = \int_{-H/2}^{H/2} \left(\frac{4(R_0 - R_{max})h^2}{H^2} + R_{max} \right)^2 dh. \tag{6}$$

Substituting $\epsilon = H/H_0 - 1$, solution of Equation (6) gives for the maximum radius

$$R_{max} = \frac{R_0}{4} \left(\sqrt{\frac{25 - 5\epsilon}{\epsilon + 1}} - 1 \right) \tag{7}$$

In Figure 2, the respective predictions of Equations (4) and (7) for the bulging of a compressed cylinder are compared. Equation (7) significantly overestimates the maximum diameter. This means that the assumption of a parabolic profile is erroneous, notwithstanding the volume correction. Equations (4) and (7) also predict different strain dependences for the bulging of bonded disks. As shown by the comparison to experimental data in Figure 3, both are in error at higher strains, with the Gent relation [Equation (4)] more accurate in compression than tension. Also, at large tensile strains, cavitation can transpire due to the presence of a triaxial state of stress,[4] introducing additional error.

In Figure 4 we plot the birefringence measured in the center of lubricated cylinders versus the true stress. From the slope at $\epsilon = 0$, we determine a stress-optical coefficient C. The results, $C = 2.07$ and $2.04\ GPa^{-1}$, for NR-1 and NR-2 respectively, are in accord with previous determinations, and also show a weak inverse dependence on crosslink density.[9] For the BR we obtain $C = 3.58\ GPa^{-1}$, which is about 15% higher than an earlier determination on a polybutadiene of similar microstructure.[10] Using these values for C, we can compare the stress present in the center of the disk with the value deduced from the applied load.

Stress–strain measurements usually refer to some average over the bulk rubber; however, from the optical birefringence, we can directly determine the difference in principal stresses developing locally in the deformed cylinder. In Figure 5 we plot the product of $C\Delta n$, where Δn was measured at $h = 0$, versus the stress calculated as the ratio of the applied force to

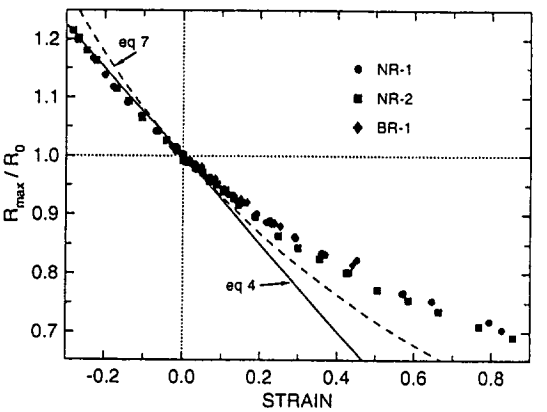

FIG. 3.—The normalized bulge radius R_{max}/R_0 of bonded disks of the three rubbers versus the imposed strain, $\epsilon = \Delta H/H_0$. Note that in agreement with theory, the profile is independent of the rubber or its modulus. Equations (4) and (7) give the same result in the limit of infinitesimal strain.

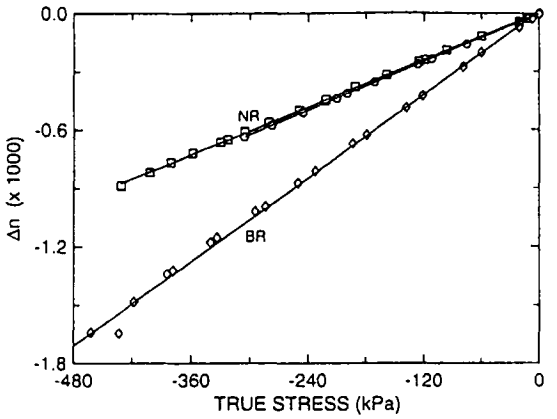

FIG. 4.—The birefringence Δn measured in the center of lubricated cylinders under compression for NR-1 (○○○), NR-2 (□□□), and BR (◇◇◇), as a function of the true stress, $\sigma = F/\pi R_{max}^2$. Note that although the difference between the NR samples is slight, there is a measurably smaller stress-optical coefficient for the more crosslinked NR-2.

the actual cross-sectional area. It is seen that the stress differences determined from the birefringence is always larger than the nominal applied stress, with the discrepancy amplified as the aspect ratio, $H_0/2R_0$, of the disk decreases. This is a direct corroboration of the idea underlying Equations (3–5) that constraints from the bonding of the cylinder generates additional stresses. Moreover, the magnitude of the additional pressure as shown in Figure 5 is very close to that given by the Gent correction [Equation (5)]. This agreement is at least in part a result of cancellation of two errors—the respective deviations of the cylinder from the shape and the volume given by Equations (3) and (4). Its flatter profile causes Equation (5) to overestimate the stresses, while the spurious volume change implicit to Equation (4) causes an underestimation of stress.

The most important feature of any geometric correction factor is the accuracy with which it converts measured data into true material properties. One way to gauge this is by comparing the stress–strain curves for the different aspect ratio cylinders of NR-2. The squatter cylinders are stiffer; however, after the correction using Equation (5), the results converge to that for the highest aspect ratio cylinder (Figure 6). In fact, for this sample, with $H_0/2R_0 = 2.3$, the

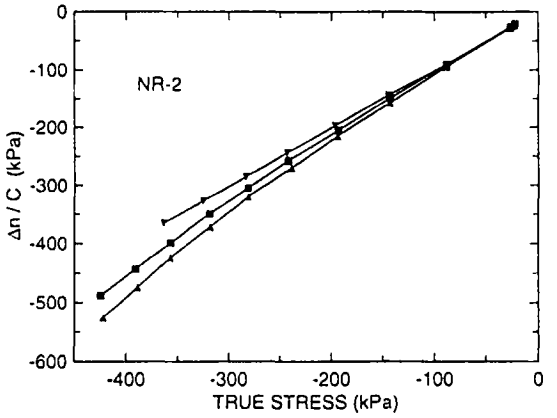

FIG. 5.—The difference in principal stresses deduced from the birefringence—using a value for the stress-optical coefficient C determined from the lubricated cylinder data in Figure (4)—versus the nominal true stress ($= F/\pi R_{max}^2$) for bonded cylinders of NR-2 having aspect ratios ($= H_0/2R_0$) equal to 0.92 (▲▲▲), 1.5 (■■■), and 2.3 (▼▼▼).

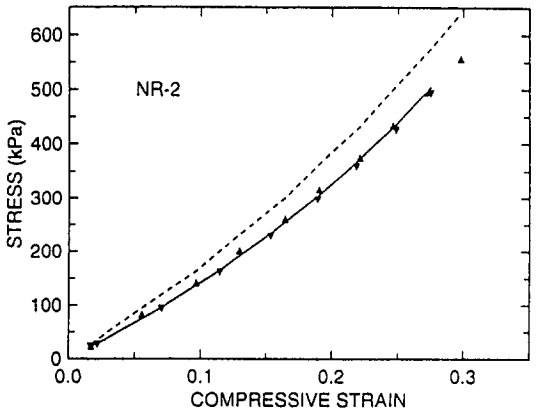

FIG. 6.—The engineering stress–strain curves for bonded cylinders of NR-2 having aspect ratios equal to 0.92 (▲▲▲) and 2.3 (▼▼▼) after correction using Equation (5). The corresponding data before correction is indicated by the dashed and solid lines, respectively. The latter differs negligibly from the data.

correction term in Equation (5) is negligible. This indicates that true material properties are obtained even for the smallest aspect ratio cylinder ($H_0/2R_0 = 0.92$) after the data is corrected.

We can also compare stress–strain results for the bonded cylinders to data obtained on the same cylinders, but lubricated at the ends so they are free to slip during compression. The measured stress–strain curves for this homogeneous compression is shown in Figure 7, along with corresponding results for bonded cylinders. After correction of the bonded cylinder data using Equation (5), the difference between the results is less than 5%. Of course, the accuracy of Equation (5) is limited by the assumption of Hookean behavior, which is only attained in rubber at low to moderate strains. (An analysis of the effects of nonlinearity on the compression of rubber blocks has been made[11,12]). Nevertheless, the error in using Equation (5) for cylinders of aspect ratios in the range from 0.92 to 2.3 is almost negligible.

SUMMARY

The behavior of rubber when subjected to different types of deformation offers rubber elasticity theorists one of their more stimulating challenges. For example, compressed rubber

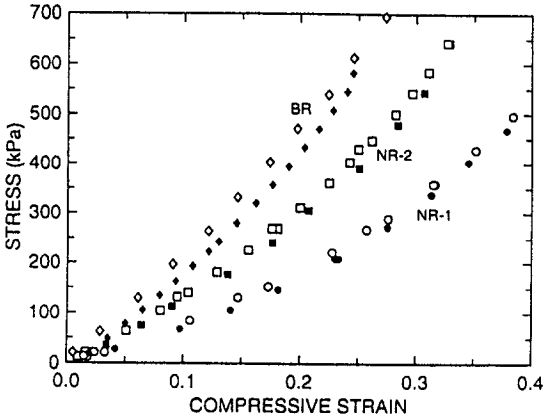

FIG. 7.—Engineering stress–strain curves measured for the two natural rubbers and the polybutadiene using lubricated (hollow points) and glued (solid points) cylinders; data for the glued cylinders were corrected according to Equation (5).

behaves almost ideally, while phenomenological treatments such as the Mooney–Rivlin model are often resorted to for a description of rubber in tension.[7,13] Another interesting issue is the stress-optical response when rubber is subjected to deformations transitioning from compression to tension. A geometry enabling these kinds of experiments is uniaxial deformation of bonded cylinders. However, in order to rely on such measurements, the correction for the nonhomogeneous strain must be accurate and reliable. The results presented herein demonstrate that any shortcomings of the Gent approach are more important in principle than in practice. The correction of the measured force–deflection data provides results in near quantitative agreement with the true material properties. Currently we are attempting to exploit experiments of this type to investigate the fundamentals of rubber elasticity.

ACKNOWLEDGMENTS

PHM expresses his gratitude for a National Research Council/ Naval Research Laboratory post-doctoral fellowship. This work was supported by the Office of Naval Research.

REFERENCES

[1] J. E. Adkins, *Proc. Cambridge Philosoph. Soc.* **50,** 334 (1954).
[2] A. N. Gent and P. B. Lindley, *Proc. Inst. Mech. Eng, London* **173,** 111 (1959).
[3] A. N. Gent, R. L. Henry, and M. L. Roxbury, *J. Appl. Mech.* **41,** 855 (1974).
[4] A. N. Gent, in "Engineering with Rubber," A. N. Gent, Ed., New York, Hanser Publishers, 1992, ch. 3.
[5] A. N. Gent, in "Science and Technology of Rubber," J. E. Mark, B. Erman, and F. R. Eirich, Eds., San Diego, Academic Press, 1994, ch. 1.
[6] A. N. Gent, RUBBER CHEM. TECHNOL. **67,** 549 (1994).
[7] L. R. G. Treloar, "The Physics of Rubber Elasticity," Oxford, Clarendon Press, 1975.
[8] E. Riande and E. Saiz, "Dipole Moments and Birefringence of Polymers," Englewood Cliffs, N.J, Prentice Hall, 1992.
[9] D. W. Saunders, *Trans. Faraday Soc.* **52,** 1414 (1956).
[10] S. Kimura, K. Osaki, and M. Kurata, *J. Polym. Sci., Polym. Phys. Ed.* **19,** 151 (1981).
[11] A. H. Muir and A. G. Thomas, *NR Technol.* **20,** 8 (1989).
[12] A. H. Muir and A. G. Thomas, *NR Technol.* **20,** 72 (1989).
[13] R. S. Rivlin, RUBBER CHEM. TECHNOL. **65,** G51 (1992).

[*Received Jun. 30, 1995; revised Jul. 31, 1995*]